*Discrete Mathematics and Theoretical Computer Science* DMTCS vol. **10:2**, 2008, 87–114

# *Neighbor discovery in multi-hop wireless networks: evaluation and dimensioning with interference considerations*[†]

Elyes Ben Hamida[1] and Guillaume Chelius[2] and Anthony Busson[3] and Eric Fleury[4]

[1]*INSA de Lyon - INRIA, 69621 Villeurbanne Cedex, France - elyes.ben-hamida@insa-lyon.fr*
[2]*INRIA - INSA de Lyon, 69621 Villeurbanne Cedex, France - guillaume.chelius@inria.fr*
[3]*IEF - CNRS, 91405 Orsay, France - anthony.busson@u-psud.fr*
[4]*ENS Lyon, 69364 Lyon, France - eric.fleury@ens-lyon.fr*

*received July 31, 2007*, *revised March 17, 2008*, *accepted May 6, 2008*.

In this paper, we study the impact of collisions and interference on a neighbor discovery process in the context of multi-hop wireless networks. We consider three models in which interference and collisions are handled in very different ways. From an ideal channel where simultaneous transmissions do not interfere, we derive an alternate channel where simultaneous transmissions are considered two-by-two under the form of collisions, to finally reach a more realistic channel where simultaneous transmissions are handled under the form of shot-noise interference. In these models, we analytically compute the link probability success between two neighbors as well as the expected number of nodes that correctly receive a `Hello` packet. Using this analysis, we show that if the neighbor discovery process is asymptotically equivalent in the three models, it offers very different behaviors locally in time. In particular, the scalability of the process is not the same depending on the way interference is handled. Finally, we apply our results to the dimensioning of a `Hello` protocol parameters. We propose a method to adapt the protocol parameters to meet application constraints on the neighbor discovery process and to minimize the protocol energy consumption.

**Keywords:** sensor networks, radio modeling, neighbor discovery, interference modeling, stochastic geometry

## 1 Introduction

### *1.1 Context*

Neighbor discovery is a key component in the communication protocol stack of multi-hop wireless networks. It is a basic service on which most of the communication protocols rely. In the context of ad hoc networks, proactive and reactive routing protocols generally use the knowledge of the nodes neighborhood to build or manage routes, *e.g.* Optimized Link State Routing (OLSR (9)) or *Ad hoc On-demand*

[†]This work is partly supported by the European Commission, project AEOLUS IST-15964, and by the CAPNET project

*Distance Vector* (AODV (25)). In sensor networks, most of the stateless routing protocols, *e.g.* Most Forward within Radius (MFR (21)) or Geographic Face Routing (GFR (7)), require the knowledge of a node neighborhood to select a next hop. Neighbor discovery is also intensively used in the context of *Delay Tolerant Networks* (DTN (18)) or *Pocket Switched Networks* (17). Based on the knowledge of contacts between entities/individuals, packet forwarding or gossiping is performed. Finally, neighbor discovery can be very useful for the study of human mobility (17) or social interactions. The interest in logging individual interactions is to compile traces in order to build models of human mobility (20) or to characterize and study dynamic graphs. Dynamic graph modeling offers a vast field of applications, covering multiple disciplines such as sociology, epidemiology, *etc*.

The neighbor discovery process is generally performed by a `Hello` protocol. A `Hello` protocol builds neighborhood tables through the periodic exchange of `Hello` messages in which a node advertises its position. The protocol generally involves several parameters such as the `Hello` packet period, its transmission power, *etc*. Some complex mechanisms like activity scheduling and the introduction of inactivity periods also interfere with the protocol characteristics and introduce new parameters to consider, like the activity/inactivity period durations. All these parameters have a real impact on the protocol performances and the discovery process: for example, neighbors can be discovered more or less rapidly and the maximum distance at which nodes can be discovered can change drastically. Energy consumption of the neighbor discovery process is also a crucial point to consider, especially in energy constraint devices such as sensor nodes or contact loggers. Finally, the radio environment has a non-negligible impact on the neighbor discovery process, particularly on the probability to discover nodes. Indeed, in real environments, radio links are never reliable and the level of interference as well as other propagation phenomena can largely reduce the protocol performances.

## 1.2 Contributions

In this paper, we take a particular look at the impact of the radio channel on the neighbor discovery process. We consider three models in which interference and collisions are handled in very different ways. From an ideal channel where simultaneous transmissions do not interfere, we derive an alternate channel where simultaneous transmissions are considered two-by-two under the form of collisions, to finally reach a more realistic channel where simultaneous transmissions are handled under the form of shot-noise interference. We prove that if the neighbor discovery process is asymptotically equivalent in these three models, it offers very different behaviors locally in time. For that, we analytically compute the link probability success between two neighbors as well as the expected number of nodes that correctly receive a `Hello` packet. Results in the three models diverge, offering different asymptotic behaviors regarding scalability for example.

Then we apply these results to the dimensioning of a `Hello` protocol parameters. The goal of dimensioning is to choose correctly the protocol parameters in order to adapt the link probability success between a node and its neighbors according to the application constraints, while minimizing the protocol energy consumption. Examples of application constraints are: "*all nodes at distance at most 10 meters must be discovered as neighbors with high probability*" or "*node at distance more than 15 meters must not be seen as neighbors*. We show how to use the analytical results to derive parameter values that respect these constraints. As a numerical application, a case study is introduced.

The remainder of this paper is organized as follows. We first reference related works in Section 2. Then, we present the considered hello protocols in Section 3 and three radio channel models are described in Section 4. The network is modeled in Section 5 and a qualitative study of the impact of interference on the neighbor discovery process is done in Section 6. The radio models are then analytically analyzed in Section 7 and compared in Section 8 . In Section 9, we discuss on the dimensioning of `Hello` protocols before concluding in Section 10.

# 2 Related works

## 2.1 Neighbor discovery

Several works have studied the design of `Hello` protocols in the context of wireless multi-hop networks. McGlynn et al (23) have proposed a family of birthday protocols which use random transmissions and node synchronization to discover the nodes adjacencies in static ad hoc networks. The proposed mathematical models as well as the simulations show the energy efficiency and the robustness of the random protocols in comparison to deterministic or scheduling algorithms.

Alonso et al (2) have provided a general model to study and analyze `Hello` protocols in ad hoc single broadcast channel networks. The time is slotted, the nodes are synchronized, in either of the two following states: listening or talking. Using this model, the authors have described and compared various `Hello` protocols. However, the model as well as the studied protocols do not consider the energy consumption. In (1), Alonso et al have extended their model to the case of ad hoc multi-channel broadcast networks.

Jakllari et al (19) have proposed a *polling-based* MAC protocol that addresses the problem of neighbor discovery with directional antennas. This type of antenna increases the capacity of the network thanks to the spatial reuse. Their protocol uses a polling strategy wherein a node polls its discovered neighbors periodically. This provides each node with the opportunity to adjust its antenna weighting coefficients in order to track its neighbors. The analytical study as well as the simulations show the efficiency of the protocol in term of capacity enhancement in the context of mobile ad hoc networks.

Vasudevan et al (27) have studied the problem of neighbor discovery in static wireless ad hoc networks with directional antennas. The proposed protocols are classified in two categories: the *Direct-Discovery* algorithms in which nodes discover their neighborhood only upon reception of a `Hello` message, and the *Gossip-Based* algorithms in which nodes also broadcast their neighbor location information. The analysis and the simulations show the efficiency of the second type of algorithms which surpasses the first one in term of adjacency discovery delay.

Most of the studies made on `Hello` protocols use rather simplistic models which do not take into account the specificities of radio communications. In our knowledge, few studies analyze the impact of interference or collisions, and more generally the impact of the radio channel modeling, on the neighbor discovery process. Few works also regard the dimensioning of the protocol with respect to interference, application constraints and energy efficiency.

## 2.2 Stochastic modeling of sensor networks

The stochastic modeling of wireless networks has already been used in various works. In particular, a general model has been introduced in (3). This model was first used to study the coverage of cellular networks (5) but was then modified and extended (4) to study properties of multi-hop wireless networks such as their capacity (13) or their *asymptotic* connectivity (11; 12; 10). In these works, stochastic geometry was often mixed with elements of the continuum percolation theory.

In this paper, we consider, apply and extend the model introduced in (4) to the context of neighbor discovery and to the performance study and dimensioning of `Hello` protocols.

# 3 The `Hello` protocols

As mentioned in Section 1, neighbor discovery is a key component of the communication protocol stack in multi-hop wireless networks such as sensor networks, delay-tolerant networks or pocket-switched networks. In most systems, this task is comitted to a `Hello` protocol which broadcasts periodically and locally a `Hello` packet to advertise the node presence.

In a `Hello` protocol, several parameters are generally involved: for example, the `Hello` packet period, its transmission power, *etc*. Some protocols can also include more complex mechanisms such as activity scheduling, thus introducing new parameters like the activity/inactivity period durations. All these parameters have an impact on the protocol performances such as the delay to discovery a neighbor, the communication range of a `Hello` packet, the energy consumption of the protocol, *etc*. The radio channel also impacts on the protocol efficiency.

To study the dimensioning of these protocols and the impact of the radio channel on the neighbor discovery process, we consider in this paper two `Hello` protocol variants. They are based on the *Aloha* (22) *Medium Access Control* (*MAC*) protocol in the sense that no *carrier sensing* nor *clear channel assessment* is performed before the transmission of a `Hello` packet. In the first `Hello` protocol, each node successively listens to the medium and transmits a `Hello` packet whereas in the second protocol, nodes can also be *sleeping*. This inactivity period is introduced to reduce the protocol energy consumption as the radio interface is turned off. We now present these two protocols in more details.

## 3.1 A basic `Hello` protocol

In the first variant, a node has two states : listening or talking. These two states occur inside a time frame, $f$, of duration $w$, as depicted on Fig.1.

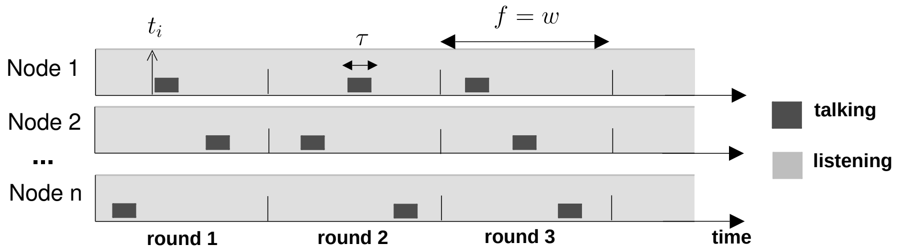


**Fig. 1:** A basic `Hello` protocol.

In each occurrence of $w$ (*a.k.a,* in each round or time frame of the `Hello` protocol), a node picks randomly an offset $t_i$, such that $t_i \in [0, w - \tau]$. The `Hello` message is then transmitted at $t_i$ during $\tau$. The `Hello` packet transmission is performed without any *carrier sensing* nor *clear channel assessment*. Each node transmits only one `Hello` message per time frame and keeps listening to the medium during the rest of the frame, for a cumulative listening duration $w - \tau$.

To briefly illustrate the impact of the protocol parameters on the neighbor discovery process, we can make a trivial reasoning. Given $\tau$ and $w$, the medium access probability is $\frac{\tau}{w}$ and the probability for a transmission not to collide with neighboring transmissions is equal to :

$$\left(1 - \frac{2\tau}{w - \tau}\right)^{n-1}$$

Where $n$ represents the number of nodes within the collision range. A fine tuning of $w$ is thus important to cope with the total number of interfering nodes $n$.

### 3.2 An energy aware `Hello` protocol

We now present a modified version of this basic `Hello` protocol including some activity scheduling. This second variant uses *sleep* periods to reduce the energy consumption in each node. During this inactivity period of duration $s$, the node radio interface is turned off. As shown on Fig.2, a node has three states : listening, talking or sleeping. These states occur inside a periodic time frame $f$ of duration $w + s$.

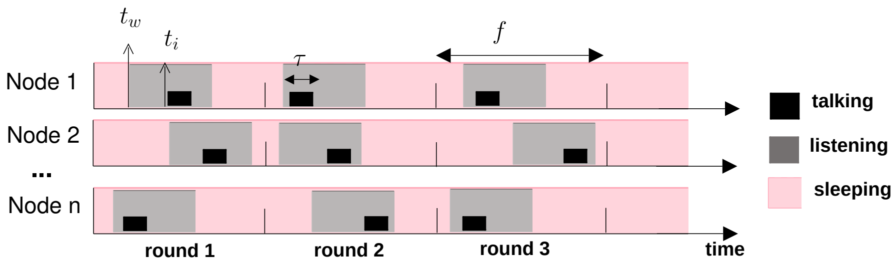


**Fig. 2:** An energy aware `Hello` protocol.

In each round of the `Hello` protocol (*i.e.,* in each occurrence of $f$), a node picks randomly an instant $t_w$, such that $t_w \in [0, s]$. Then, the node picks randomly a second instant $t_i$, such that $t_i \in [t_w, t_w + w - \tau]$. The `Hello` message is transmitted at $t_i$ with a duration of $\tau$.

Hereby, a node is in the talking state during $[t_i, t_i + \tau]$, in the listening state during $[t_w, t_w + w] \setminus [t_i, t_i + \tau]$ and in the sleeping state during the rest of the frame $f$. In the sleeping state, the radio interface is off and the node can not receive any message. To sum up, for each occurrence of $f$, a node transmits only one message with a duration of $\tau$, listens to the medium during $w - \tau$ and sleeps during $s$.

To continue with the trivial reasoning started in the previous section, the medium access probability is now $\frac{\tau}{w+s}$ and the probability to discover a given node is equal to:

$$\frac{w - \tau}{w + s}\left(1 - \frac{2\tau}{w + s}\right)^{n-2}$$

Where $n$ is the total number of nodes within the collision range. In this variant, two parameters, $w$ and $s$, have to be well tuned in order to increase the probability for a node to discover its neighbors.

## 4 The radio channel

From a network point of view, a radio channel model aims at predicting the transmission error probability associated with each radio link. A radio link relies on the transmitter and receiver positions but depends also on many parameters and phenomena such as path-loss, shadowing, fading, modulation or interference, *etc*.

At a given location $x$ ($x \in I\!R^2$), the signal strength for an emission from node $X_i$ is $S_i l(\|X_i - x\|)$ where $\|.\|$ is the Euclidean norm in $I\!R^2$, $S_i$ is the emission power of $X_i$ and $l(.)$ is the path-loss function. $l(.)$ is a decreasing function from $I\!R^+$ in $I\!R^+$ which models the attenuation of the signal strength with regard to the distance. Many different functions have been proposed in the literature for $l(.)$. As an example, the path-loss is classically modeled using a power-law function as in the Friis formula (14):

$$l(u) = A_0.u^{-\beta}$$

Where $A_0$ is a constant depending on the frequency and the antenna gain, and $\beta$ is a parametric path-loss exponent introduced to fit various environments and typically ranging from 2.0 to 6.0. In the original Friis formula, we have $\beta = 2$.

However, mathematical problems may arise due to the divergence of this function near 0. Basically, this formula is valid in far field only. To avoid any problem occurring near the transmitter when the node intensity increases, several bounded functions have been introduced. As examples, (10; 6) propose the following path-loss functions:

$$\begin{aligned} l(u) &= A_0.min(1, u^{-\beta}) \\ l(u) &= A_0.(1+u)^{-\beta} \\ l(u) &= A_0.\frac{1}{1+u^{\beta}} \end{aligned}$$

When it will not be specified, we will consider $l(.)$ to be a generic decreasing function. However, we will also consider $l(u) = \frac{1}{C+u^{\beta}}$, with $C \in I\!R^+$ and $\beta \geq 2$.

## 4.1 *The* ideal *model*

In a first time, we consider a very simple radio channel model where interference is not considered. We assume that a transmission is received if its *signal to noise ratio* (*snr*) is above a given constant $\theta$ function of the transmission data-rate. This view is inherited from the field of information theory and the Shannon's law. Given this model, an emission from node $X_i$ is correctly received at location $x$ if:

$$snr(X_i, x) = \frac{S_i l(\|X_i - x\|)}{W_x} > \theta \qquad (1)$$

Where $W_x$ in $I\!R^+$ models the ground noise level at the location $x$.

As $l(.)$ is decreasing and for a constant noise $W_x$, this model results into a perfect circular coverage area around each node with a maximal communication range $R(S_i)$ defined as follows:

$$R(S_i) = \sup\{r \in I\!R^+ | \frac{S_i l(r)}{W_x} > \theta\} \qquad (2)$$

Thus, a node $X_i$ can send frames only to nodes within its communication area $\mathcal{B}(X_i, R(S_i))$, *i.e.*, the open ball of radius $R(S_i)$ centered on $X_i$. A node $x$ is said to be covered by $X_i$ if it lies within $X_i$ communication area.

### 4.2 *The* collision *model*

We define a radio channel model where interference is partially considered under the form of collisions. We still assume that a transmission can be received if its snr is above $\theta$ but we also suppose that a simultaneous communication initiated by node $X_j$ collides with the transmission of $X_i$ if:

$$snr(X_j, x) > \delta snr(X_i, x) \tag{3}$$

With $\delta \in I\!R^+$. When suffering a collision, we assume that a transmission is lost.

We can note that this model is a generalization of the *Protocol model* described in (16). Indeed, formula 3 can be rewritten as follows:

$$\begin{aligned} snr(X_j, x) &> \delta snr(X_i, x) \\ \Leftrightarrow \frac{S_j l(\|X_j - x\|)}{W_x} &> \delta \frac{S_i l(\|X_i - x\|)}{W_x} \\ \Leftrightarrow S_j l(\|X_j - x\|) &> \delta S_i l(\|X_i - x\|) \end{aligned}$$

As $l(.)$ is decreasing and under the assumption of a constant emission power for all nodes, we obtain the condition given by the *Protocol model* in (16).

### 4.3 *The* SINR *model*

We finally present a more realistic radio model where perturbations steaming from all concurrent transmissions are considered simultaneously when evaluating the correct reception of a frame. A frame from $X_i$ can be correctly received at a location $x$ if and only if the frame *Signal to Interference and Noise Ratio*, the so-called *SINR*, at location $x$ is above a given threshold $\theta$.

$$sinr(X_i, x) = \frac{S_i l(\|X_i - x\|)}{W_x + I(x)} > \theta \tag{4}$$

Where $W_x$ in $I\!R^+$ still models the ground noise level at the location $x$ and $I(x)$ is the *shot-noise* interference, *i.e.*, the sum of all simultaneous transmission signal strengths:

$$I(x) = \sum_{X_j \in \Gamma, X_j \neq X_i} S_j l(\|X_j - x\|)$$

Where $\Gamma$ is the set of simultaneous emitters. This model is similar to the CDMA model introduced in (4) with a correlation factor $\gamma = 1$. It supposes that the interference is Gaussian. This assumption holds in the case of a high number of interfering nodes and in the absence of a preponderant interferer. In practice, with most systems, 3 to 4 interferers are enough for the interference to be Gaussian. In the other cases, it is not valid (28) and a precise study of the interference impact would require to enter into details and precisely specify the radio interface characteristics, *e.g.* its modulation. In order to keep a high level of abstraction, we rather consider a Gaussian interference. This assumption is also acceptable regarding the two following remarks: first, we consider a large network where the number of simultaneous emissions is important. Second, in the case of a preponderant interferer, the communication would no succeed, whatever the interference model. Indeed, we consider single resource radio systems with no multi-user mechanisms such as CDMA.

### 4.4 Fading & shadowing

The path-loss function $l(.)$ predicts the mean received power at a given distance and leads to disk coverage areas. It is obvious that strong variations can be experienced by real nodes owing to the real environment. It is usual to classify these effects in two main categories: shadowing and fading.

Shadowing relies on large scale signal variations due to obstacles in the environment. These large scale variations are introduced thanks to a multiplicative random noise. This noise is generally modeled using a log-normal law. Note that this function stands for static variations around the isotropic mean function.

In severe environments, with multiple obstacles and walls, wave propagation generates several paths between the transmitter and the receiver. The received signal thus issued from an incoherent summation of several components becomes a random variable and is subject to fading. In this case, the received signal is still corrupted by a multiplicative noise. In the case of the most severe conditions, referred to as a *Rayleigh* channel, the statistics of the signal's amplitude becomes a random exponential variable of parameter $\mu$.

From a network point of view, the leading difference between shadowing and fading is that shadowing introduces a static alteration of the isotropic determinist power prediction while fading introduces received power variations from frame to frame.

To handle the shadowing and fading phenomena, we do not consider the sequence $(S_i)_{i=1,2,..}$ as a sequence of deterministic values but rather as a sequence of random variables in $\mathbb{R}^+$ independently and identically distributed. If not explicitly specified, we will suppose that the $S_i$ follow a generic distribution. However, we will also consider the special case of a *Rayleigh* channel where the $S_i$ follow an exponential distribution.

In reality fading and shadowing are emitters and receivers dependent. It means that for a given emitter, the fading are different with regard to the locations of the receivers. But, for the quantities we are studying, we consider only the signal power received by a typical node (at a given location). Therefore, without loss of generality, fading and shadowing can be modeled by two random variables associated to each node.

## 5 Stochastic modeling of the network

In order to study and dimension the neighbor discovery process, we use a stochastic modeling of the network. This approach is interesting as it permits to reduce the complexity of the study and in particular the number of variables, such as the location of each node, to a single parameter, the intensity of the point process used to model the nodes location. Stochastic modeling provides useful hints on the macroscopic and average behavior of the network.

### 5.1 Location model

We consider a network made of nodes dispatched in a two-dimensional geographical region. We assume that location of nodes is modelled by a stationary Poisson point process $\Phi_0$ of constant spatial intensity $\lambda_0$ (the mean number of nodes per unit area). With such a process, the number of points lying in a region $B$ of the plane follows a discrete Poisson law, and given the number of points in $B$, nodes are independently and uniformly distributed in $B$.

If $\Phi_0(B)$ is the random variable which counts the number of points lying in $B$, we have:

$$\mathbb{P}\left(\Phi_0(B) = k\right) = \frac{(\lambda_0|B|)^k}{k!} e^{-\lambda_0|B|}$$

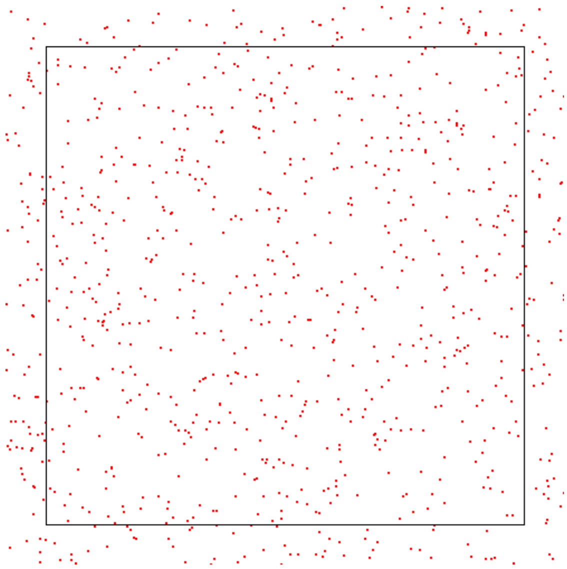

**Fig. 3:** Realization of a Poisson point process of intensity $\lambda = 0.0035$ in a $500 * 500$ square region.

Where $k$ is a positive integer and $|.|$ is the Lebesgue measure in $I\!R^2$. As an illustration, a realization of a Poisson point process of intensity $\lambda = 0.0035$ is given in Figure 3.

## 5.2 Application model

Given the description of the `Hello` protocols presented in Section 3, the nodes of $\Phi_0$ are split in two subsets, the active and the sleeping nodes. Each node is active with probability $q$ independently of the other nodes. The set of active nodes is a thinning of the point process $\Phi_0$ which leads to a stationary Poisson point process $\Phi_1$ with intensity $\lambda_1 = q\lambda_0$. An active node is emitting with probability $p$ independently of the other nodes. It leads to a new thinning of the point process $\Phi_1$. Let denote $\Phi_2$, the point process modeling the emitters. $\Phi_2$ is a stationary Poisson point process with intensity $\lambda_2 = p\lambda_1 = qp\lambda_0$. If we inject the parameters associated to the `Hello` protocols of Section 3, we have $p = \frac{\tau}{w}$, $q = 1$ for the protocol without *sleep* periods and $p = \frac{\tau}{w}$, $q = \frac{w}{w+s}$ for the one with *sleep* periods.

The values of $p$ and $q$ correspond to a simplification with regard to the `Hello` protocol. First, we have neglected the border effect. Indeed, if a node picks its emitting time at the beginning or at the end of the slot, its collision probability gets smaller. Second, $\Phi_2$ represents the nodes which emission overlap with the considered one. In practical, the nodes being non-synchronized, this overlapping is mainly partially and does not last for the whole transmission. However, in order to simplify our model, we do not take into account the variation of the interference stemming from the other nodes. In other words, we assume that each overlap affect the whole transmission of the `Hello` frame. In a way, it leads to a worst case analysis. These simplifications can be easily changed. For instance, the parameters $p$ and $q$ can also be chosen in such a way they represent the mean number of interfering nodes during a transmission. In fact, there is no particular assumptions on the values of $p$ and $q$ (except that $0 < p, q \leq 1$ and that the process $\Phi_2$ must be an independent thinning of $\Phi_0$).

# 6 Impact of interference on neighbor discovery

Now that we have modeled both the network and the radio channel, we can start looking at the impact of interference on the neighbor discovery process. To begin with, we make a short qualitative study by giving an illustration of the logical network topology built by the `Hello` protocol and as observed by the nodes. We introduce the notion of logical connectivity graph in opposition to the physical connectivity graph. Then, we illustrate the impact of the different radio channel models presented in Section 4 on this logical connectivity graph.

## 6.1 Graph of connectivity

During the process of neighbor discovery, *i.e.*, the execution of the `Hello` protocol, when a `Hello` packet is received, the identity of the emitter is added to the neighborhood table of the receiving node. From the tables of all nodes, we can extract a graph of logical connectivity as it is observed by the nodes. The graph is composed of the adjacencies that the nodes have discovered. This notion of connectivity is *logical* as it is built upon the reception of packets as opposed to a *physical* connectivity which would only rely on the physical medium characteristics. In other terms, interference and collisions affect the logical connectivity as they affect the correct reception of `Hello` packets.

Contrarily to a physical connectivity graph, the logical connectivity graph is dynamic. Indeed, due to the non-deterministic nature of the `Hello` protocol, new adjacencies may be observed as the neighbor discovery process keeps on being executed. The logical connectivity graph is thus the sum of all adjacencies observed up to a given instant. In the next section, to simplify the discussion but without loss of generality, we will decompose the time in rounds of the `Hello` protocol.

## 6.2 Impact of the radio channel model

We have simulated the basic `Hello` protocol described in Section 3.1 according to the three radio channel models presented in Section 4 (*i.e.*, the *ideal* model, the *collision* model and the *sinr* model). The objective is to qualitatively study the number of nodes discovered during the different rounds of the `Hello` protocol. As for each node and each round, the instant $t_i$ of the `Hello` packet transmission changes, one can expect to discover new neighbors at each round of the protocol.

The graphs of logical connectivity obtained for the *ideal* radio model is plotted on Figures 4(a), while in Figures 4(b) and (c), we show the *collision* radio model. In Figures 4(b) we consider a collision range equal to the transmission range and in Figures 4(c) this range is twice the coverage radius. Finally, results obtained for the *sinr* radio model are depicted on Figures 4(d).

First, we notice on Figure 4(a) that in the *ideal* radio model, all nodes within transmission range are discovered during the first round. This resulting graph of logical connectivity is not realistic as no collision nor interference occur. If high level protocols are built assuming an ideal underlaying radio model, we can have doubts about their proper functioning in real environments.

Second, from Figures 4(b), we can observe that collisions affect the logical graph of connectivity as numerous adjacencies are not discovered. If in each round, new neighbors are discovered, their total number remains lower than the number of nodes present within the transmission range of each node, even after 3 rounds of the `Hello` protocol. In Figures 4(c), the collision range is twice the transmission range. The impact of collisions increases and, as a consequence, the number of discovered adjacencies is largely reduced. However, in both cases, we notice that long links are sometimes established. This suggests that in the *collision* model, the distance between two nodes does not strongly restrict the neighbor discovery.

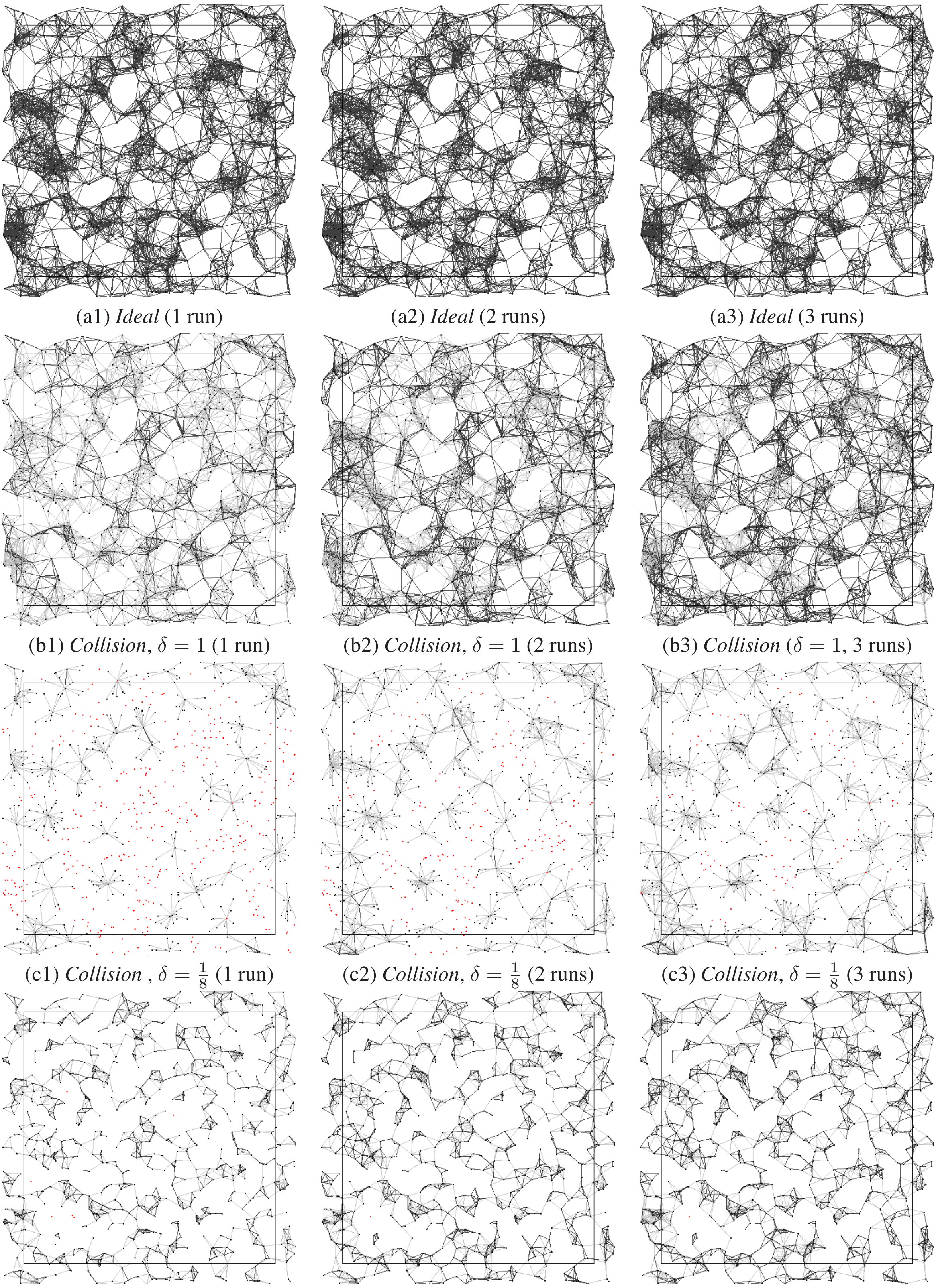

(a1) *Ideal* (1 run) (a2) *Ideal* (2 runs) (a3) *Ideal* (3 runs)

(b1) *Collision*, $\delta = 1$ (1 run) (b2) *Collision*, $\delta = 1$ (2 runs) (b3) *Collision* ($\delta = 1$, 3 runs)

(c1) *Collision* , $\delta = \frac{1}{8}$ (1 run) (c2) *Collision*, $\delta = \frac{1}{8}$ (2 runs) (c3) *Collision*, $\delta = \frac{1}{8}$ (3 runs)

(d1) *SINR* (1 run) (d2) *SINR* (2 runs) (d3) *SINR* (3 runs)

**Fig. 4:** Logical connectivity graphs for various radio channel models ($w = 200$, $\tau = 10$, $s = 0$, $\lambda = 0.0035$, $S = 50000$, $\theta = 1$, $\beta = 3$, $W = 1$).

The graphs of connectivity resulting from the *sinr* model are shown on Figure 4(d). As for the *collision* model, the number of discovered neighbors is lower than the number of nodes present within transmission range of each node, even after 3 rounds. Furthermore we observe that in this model, only short links are established. This suggests clearly that in the *sinr* model, the distance has a stronger impact on the discovery process than in the *collision* one.

This qualitative study shows the importance of considering interference and collisions while designing and evaluating communication protocols. Thereby, in the rest of this paper, we will study the radio link success probability depending on the considered radio channel model. We will use later this analysis for the dimensioning of the neighbor discover process.

# 7 Analysis of the radio link

Now that we have highlighted the impact of the radio channel model on the neighbor discovery process, we perform an analysis of a given radio link depending on the way collisions and interference are handled.

In this section as well as in the following ones, in order to compute the probability that a transmission succeeds as well as the average number of successful receptions for a given packet, we consider a particular emitter and receiver. The emitter is located at the origin and is named $O$. The emission power for this node is $S$ and follows the same distribution as the random variables $(S_i)_{i=1,2,\ldots}$. The receiver is located at $y$ ($y \in \mathbb{R}^2$) and $W$ is the ground noise level at location $y$. The distance between the two nodes is denoted $r$ ($\|y\| = r$). These two points are added to the points of $\Phi_0$.

## 7.1 *Analysis of the* ideal *channel*

We first study the *ideal* channel where no collision nor interference occur. Let $p(r)$ be the probability that a frame from $O$ is correctly received by $y$. In this particular channel, we have:

$$p(r) = \begin{cases} 1 \text{ if } r < R(S) \\ 0 \text{ otherwise} \end{cases}$$

Let us call $N$ the random variable denoting the number of nodes that correctly receive the frame from $O$. As transmitting and sleeping nodes have their radio interface busy or off, the point process of potential receivers is a Poisson point process of intensity $\lambda_1 - \lambda_2 = (1-p)\lambda_1$. Trivially, we have

$$\mathbb{E}[N] \quad = \quad (1-p)q\lambda_0\pi R(S)^2$$

If we consider the particular path-loss function $l(u) = \frac{1}{C+u^\beta}$ introduced in section 4, we obtain:

$$p(r) = \begin{cases} 1 \text{ if } r < \sqrt[\beta]{\frac{S}{W\theta} - C} \\ 0 \text{ otherwise} \end{cases} \tag{5}$$

The average number of successful receptions can be written as follows:

$$\mathbb{E}[N] \quad = \quad (1-p)q\lambda_0\pi\left(\frac{S}{W\theta} - C\right)^{\frac{2}{\beta}} \tag{6}$$

## 7.2 *Analysis of the* collision *channel*

We now leave the ideal case and lightly refine the radio channel to handle collisions using the *collision* model given in section 4.2. We also assume that all nodes transmit at a constant power and we do not consider shadowing nor fading. We still consider a transmission between node $O$ and node $y$.

### 7.2.1 *Link success probability*

Given the inequality 3, a collision with another transmission initiated by $X_j$ occurs if:

$$\begin{aligned} snr(X_j, y) &> \delta snr(O, y) \\ \Leftrightarrow l(\|X_j - y\|) &> \delta l(r) \end{aligned}$$

Still considering the particular path-loss function $l(u) = \frac{1}{C+u^\beta}$ introduced in section 4, the condition becomes:

$$\begin{aligned} snr(X_j, y) &> \delta snr(O, y) \\ \Leftrightarrow l(\|X_j - y\|) &> \delta l(r) \\ \Leftrightarrow \|X_j - y\|) &< \sqrt[\beta]{\frac{(1-\delta)C + r^\beta}{\delta}} \end{aligned}$$

Thus, $p(r)$ can be expressed as:

$$p(r) \;=\; \mathbb{P}\left(\Phi_2\left(\mathcal{B}\left(y, \sqrt[\beta]{\frac{(1-\delta)C + r^\beta}{\delta}}\right)\right) = 0\right)$$

Where $\mathcal{B}(y, r)$ is the ball of radius $r$ centered around $y$. Finally, $p(r)$ can be written as:

$$p(r) = \begin{cases} e^{-pq\lambda_0\pi\left(\frac{(1-\delta)C+r^\beta}{\delta}\right)^{\frac{2}{\beta}}} & \text{if } r < \sqrt[\beta]{\frac{S}{W\theta} - C} \\ 0 \quad \text{otherwise} \end{cases} \tag{7}$$

### 7.2.2 *Mean number of successful receptions*

According to the Campbell theorem, the mean number of nodes $N$ which correctly receive the frame is:

$$\begin{aligned} \mathbb{E}\left[N\right] &= \mathbb{E}\left[\sum_{X_i \in I\!R^2} 1\!\!1_{\forall X_j \in \Phi_2, \|X_j - x\| \geq \sqrt[\beta]{\frac{(1-\delta)C + \|x\|^\beta}{\delta}}} dx\right] \\ &= (1-p)q\lambda_0 \int_{I\!R^2} \mathbb{E}^0_{\Phi_1}\left[1\!\!1_{\forall X_j \in \Phi_2, \|X_j - x\| \geq \sqrt[\beta]{\frac{(1-\delta)C + \|x\|^\beta}{\delta}}}\right] dx \\ &= (1-p)q\lambda_0 \int_{I\!R^2} \mathbb{P}\left(\forall X_j \in \Phi_2, \|X_j - x\| \geq \sqrt[\beta]{\frac{(1-\delta)C + x^\beta}{\delta}}\right) dx \\ &= (1-p)q\lambda_0 2\pi \int_0^{+\infty} p(r) r dr \end{aligned}$$

Where $\mathbb{E}^0_{\Phi_1}[.]$ is the expectation under the Palm measure with regard to the process $\Phi_1$ (see (26) page 119 for more details). Finally $\mathbb{E}[N]$ is written as :

$$\mathbb{E}[N] = (1-p)q\lambda_0 2\pi \int_0^{\sqrt[\beta]{\frac{S}{W\theta}-C}} e^{-pq\lambda_0\pi\left(\frac{(1-\delta)C+r^\beta}{\delta}\right)^{\frac{2}{\beta}}} r\, dr$$

If we assume that the collision area is equal to the transmission range (i.e., $\delta = 1$), then $\mathbb{E}[N]$ can be expressed as :

$$\begin{aligned}
\mathbb{E}[N] &= (1-p)q\lambda_0 2\pi \int_0^{\sqrt[\beta]{\frac{S}{W\theta}-C}} e^{-pq\lambda_0\pi r^2} r\, dr \\
&= (1-p)\lambda_1 \left[-\frac{e^{-pq\lambda_0\pi r^2}}{pq\lambda_0}\right]_0^{\sqrt[\beta]{\frac{S}{W\theta}-C}} \\
&= \frac{(1-p)q\lambda_0}{pq\lambda_0}\left[1-e^{-pq\lambda_0\pi\left(\frac{S}{W\theta}-C\right)^{\frac{2}{\beta}}}\right] \\
&= \frac{1-p}{p}\left[1-e^{-pq\lambda_0\pi\left(\frac{S}{W\theta}-C\right)^{\frac{2}{\beta}}}\right] \qquad (8)
\end{aligned}$$

### 7.3 *Analysis of the* SINR *channel*

We finally analyse the most realistic model where a frame from $O$ is correctly received by a node $y$ if and only if the *Signal to Interference and Noise Ratio* at $y$ is above a given threshold $\theta$:

$$p(r) = \mathbb{P}\left(\frac{Sl(r)}{W+I_{\Phi_2}(y)} > \theta\right) \qquad (9)$$

The random variable $I_{\Phi_2}(y)$ represents the interference generated by the other emitters. $I_{\Phi_2}(y)$ is the sum of the signal strengths at $y$ from all simultaneous transmissions:

$$I_{\Phi_2}(y) = \sum_{X_i\in\Phi_2} S_i l(\|X_i - y\|)$$

Note that as the marks $S_i$ are identically distributed, they do not depend on location of nodes. Consequently, the distribution of $I_{\Phi_2}(y)$ does not depend on $y$.

#### 7.3.1 *Link success probability*

In order to increase the realism of the model and to study its impact on the radio link, we consider here a *Rayleigh* channel. In consequence, the sequence of random variables $(S_i)_{i=1,2,..}$ follow exponential laws with parameter $\mu$. The mean emission power of a node is then $\frac{1}{\mu}$. Equation (9) can be rewritten as:

$$p(r) = \mathbb{P}\left(S > \frac{\theta}{l(r)}\left(W + I_{\Phi_2}(y)\right)\right)$$

As $S$ is exponentially distributed, $\mathbb{P}(S > x) = e^{-\mu x}$ for $x > 0$ and conditioning by the values of $W$ and $I_{\Phi_2}(y)$, we get

$$\begin{aligned} p(r) &= \mathbb{E}\left[e^{-\mu\frac{\theta}{l(r)}\left(W + I_{\Phi_2}(y)\right)}\right] \\ &= \mathbb{E}\left[e^{-\mu\frac{\theta}{l(r)}W}\right]\mathbb{E}\left[e^{-\mu\frac{\theta}{l(r)}I_{\Phi_2}(y)}\right] \end{aligned} \tag{10}$$

The last expression depends on the Laplace transform of $I_{\Phi_2}(y)$. Fortunately, a close form expression for it is known. Without loss of generality we compute the Laplace transform at the origin rather than at $y$. Remember that the distribution of $I_{\Phi_2}(y)$ does not depend on $y$. The Laplace transform $L_{I_{\Phi_2}}(0)$ of $I_{\Phi_2}(0)$ is defined as

$$L_{I_{\Phi_2}(O)} = \mathbb{E}\left[e^{-sI_{\Phi}(O)}\right]$$

When the emission power of a node follows an exponential law and for $l(r) = \frac{1}{C + r^{\beta}}$, we get:

$$\begin{aligned} L_{I_{\Phi_2}(O)} &= \mathbb{E}\left[e^{-s\sum_{X_i\in\Phi_2} S_i l(\|X_i\|)}\right] \\ &= \mathbb{E}\left[\prod_{X_i\in\Phi_2} e^{-sS_i l(\|X_i\|)}\right] \end{aligned}$$

Classical arguments of stochastic geometry (see for instance the generating functional of a Poisson point process in (26) pages 115-116) lead to:

$$\begin{aligned} L_{I_{\Phi_2}(O)} &= e^{-\lambda_2\int_{\mathbb{R}^2}\left(1 - \mathbb{E}\left[e^{-sS_1 l(\|x\|)}\right]\right)dx} \\ &= e^{-\lambda_2\int_0^{+\infty}\left(1 - \mathbb{E}\left[e^{-sS_1 l(u)}\right]\right)udu} \\ &= e^{-\lambda_2 2\pi\int_0^{+\infty}\left(1 - \frac{\mu}{\mu + sl(u)}\right)udu} \\ &= e^{-\lambda_2 2\pi\left(\int_0^{+\infty}\frac{s}{\mu(C+u^{\beta})+s}\right)udu} \\ &= e^{-\lambda_2 2\pi^2\frac{s(\mu C+s)^{\frac{2}{\beta}-1}}{\beta sin\left(\frac{2\pi}{\beta}\right)\mu^{\frac{2}{\beta}}}} \end{aligned} \tag{11}$$

If we suppose that the noise $W$ is constant, and combining equations (10) and (11), the probability $p(r)$ becomes:

$$\begin{aligned} p(r) &= e^{-\mu\frac{\theta}{l(r)}W} L_{I_{\Phi}(O)}\left(\mu\frac{\theta}{l(r)}\right) \\ &= e^{-\mu\frac{\theta}{l(r)}W} e^{-\lambda_2 2\pi^2\frac{\mu\frac{\theta}{l(r)}\left(\mu C+\mu\frac{\theta}{l(r)}\right)^{\frac{2}{\beta}-1}}{\beta sin\left(\frac{2\pi}{\beta}\right)\mu^{\frac{2}{\beta}}}} \\ &= e^{-\mu\theta(C+r^{\beta})W} e^{-\lambda_2 2\pi^2\frac{\theta(C+r^{\beta})\left(C+\theta(C+r^{\beta})\right)^{\frac{2}{\beta}-1}}{\beta sin\left(\frac{2\pi}{\beta}\right)}} \end{aligned} \tag{12}$$

We note that if the noise is nil ($W = 0$), the probability $p(r)$ does not depend on the emitting power. Increasing or decreasing the emission power increases or decreases the interference proportionally in such a way that the *SINR* remains constant.

### 7.3.2 Mean number of successful receptions

According to the Campbell theorem, the mean number of nodes $N$ which correctly receive the frame is:

$$\begin{aligned}
\mathbb{E}[N] &= \mathbb{E}\left[\sum_{X_i \in \mathbb{R}^2} \mathbb{1}_{\frac{Sl(\|x\|)}{W+I_{\Phi_2}(x)}>\theta} dx\right] \\
&= (1-p)\lambda_1 \int_{\mathbb{R}^2} \mathbb{E}^0_{\Phi_1}\left[\mathbb{1}_{\frac{Sl(\|x\|)}{W+I_{\Phi_2}(x)}>\theta}\right] dx \\
&= (1-p)\lambda_1 \int_{\mathbb{R}^2} \mathbb{P}\left(\frac{Sl(\|x\|)}{W+I_{\Phi_2}(x)} > \theta\right) dx \\
&= (1-p)\lambda_1 2\pi \int_0^{+\infty} p(r) r dr
\end{aligned} \tag{13}$$

In the general case, the integration of $p(r)$ is difficult but can be resolved numerically using a Riemann sum.

# 8 Discussion on the radio link model

After the qualitative discussion of Section 6 and the analysis done in Section 7, we can now precisely study the impact of the radio model on the neighbor discover process. A first result is that after an infinite number of rounds, the logical connectivity graphs build in the three models are equal. However, if they are asymptotically equivalent, the models offer very different behavior over a short period of time. This will be shown through the comparison of $p(r)$ and $\mathbb{E}[N]$.

## 8.1 Convergence of the logical connectivity graphs

We suppose here that $\Phi_0$ is a homogeneous Poisson point process and $(S_i)_{i=1,2,..}$ are constant and equal to $S$. Let $\mathcal{G}(\Phi_0, R(S))$ be the graph made of the elements of $\Phi_0$ with an edge between $x, y \in \Phi_0$ if and only if $\|x - y\| < R(S)$. Let $\mathcal{G}^i_t(\Phi_0)$, $\mathcal{G}^c_t(\Phi_0)$ and $\mathcal{G}^s_t(\Phi_0)$ be the logical connectivity graphs built by the neighbor discovery process after $t$ rounds in the *ideal*, *collision* and *sinr* models respectively. More generally, for a generic radio model $m$, $\mathcal{G}^m_t(\Phi_0)$ contains all the adjacencies that have been discovered by the execution of the `Hello` protocol during $t$ rounds in the radio model $m$. We define:

$$\lim_{t\to+\infty} \mathcal{G}^m_t(\Phi_0) = \mathcal{G}^m_\infty(\Phi_0)$$

**theorem 1** *If* $0 < p < 1$ *and* $0 < q \leq 1$*, we have:*

$$\mathcal{G}(\Phi_0, R(S)) = \mathcal{G}^i_\infty(\Phi_0) = \mathcal{G}^c_\infty(\Phi_0) = \mathcal{G}^s_\infty(\Phi_0)$$

**Proof:** We consider a particular sample of the homogeneous Poisson point process $\Phi_0$. Let $x, y$ two points of $\Phi_0$. Suppose that the edge $(x, y)$ is not in $\mathcal{G}(\Phi_0, R(S))$. By definition, we have $\|x - y\| \geq R(S)$ and thus $p(\|x - y\|) = 0$ in all three radio models. Trivially, we can say that whichever $t \in I\!N$, the edge does not belong to $\mathcal{G}_t^i(\Phi_0)$, $\mathcal{G}_t^c(\Phi_0)$ or $\mathcal{G}_t^s(\Phi_0)$.

Suppose now that $(x, y)$ is in $\mathcal{G}(\Phi_0, R(S))$, *i.e.* $\|x - y\| < R(S)$. We want to prove that $(x, y)$ is in $\mathcal{G}_\infty^m(\Phi_0)$ with $m$ being one the three considered models. Let $A(n)$ be the event that the adjacency $(x, y)$ is observed during the round $n$. Clearly the $(A(n))_{n=1,2...}$ are independent (given $\Phi_0$ and for $S_i = S\ \forall i$). Moreover, $\forall (i, n), \mathbb{P}(A_n) = \mathbb{P}(A_i)$. Thanks to the *Borel-Cantelli* lemma, in order to show that $(x, y)$ is in $\mathcal{G}_\infty^m(\Phi_0)$, it is sufficient to show that $\sum_{n=1}^{\infty} \mathbb{P}(A_n) = \infty$.

Whichever model is considered, we have $\mathbb{P}(A_n) = p(\|x - y\||\Phi_0)q(1 - p)$ where $p(r|\Phi_0)$ is the probability of success when the distance between the emitter and the receiver is $r$ and given $\Phi_0$. It is thus sufficient to prove that $p(\|x - y\||\Phi_0) > 0$. It is clearly the case in the *ideal* and *collision* models as $\|x - y\| < R(S)$. For the *sinr* model, it is a bit more complicated.

Let $I_d(\Phi_0(y))$ be the interference stemming from all the nodes of $\Phi_0$ located outside the ball of radius $d$ centered on $y$. For the path-loss presented in Section 4 and since $\Phi_0$ is a Poisson point process, the interference $I(\Phi_0(y))$ is almost surely finite. Therefore, for all $\epsilon > 0$ it exists almost surely a finite distance $d$ such that the probability that $\{I_d(\Phi_0(y)) < \epsilon\}$ is strictly positive.

So we have a strictly positive probability to have an interference level coming from outside of $\mathcal{B}(y, d)$ inferior to $\epsilon$. Moreover, we have a strictly positive probability to have no interference coming from inside $\mathcal{B}(y, d)$ as $\Phi_0(\mathcal{B}(y, d))$ is finite (since $d$ is almost surely finite). Since $I_d(\Phi_2(y)) \leq I_d(\Phi_0(y))$, this result also holds for $I_d(\Phi_2(y))$ even if $\Phi_2$ is not an independent thinning of $\Phi_0$.

As the product of these two probabilities is an inferior bound to $p(\|x - y\||\Phi_0)$, the probability for the adjacency to be observed is thus strictly positive.

This result can be extended to the case where the random variables of the sequence $(S_i)_i$ are randomly distributed (but in such a way that $I_\Phi$ is almost surely finite). We have to prove that, for the *sinr* model, a link observed in the $\mathcal{G}_t^i(\Phi_0)$ or $\mathcal{G}_t^c(\Phi_0)$ graphs has a positive probability to be observed during a slot. If we suppose that $S_i$ varies in time but that they are independent in each slot, the same proof holds. If we suppose that $S_i$ does not vary in time, the same line as the proof applied to $\mathbb{P}(A_n) = p(\|x - y\||\Phi_0, (S_i)_i)$ leads to the result.

□

This result is interesting as it says that whichever radio model is used, *at the end*, the neighbor discovery process leads to the same connectivity graph. However, this asymptotic notion is problematic as the number of rounds required to reach this convergence can be infinite. During the real execution of the discover process, *i.e.* after a finite number of rounds, the obtained logical connectivity graphs can largely vary as observed in Section 6. We will show in the next Section that the radio link properties also largely vary.

## 8.2 Radio link probability

If the different models asymptotically lead to the same logical connectivity graph, they have really different behaviors. As an example, the distributions of $p(r)$ are different depending on the radio model. Figure 5 compares the link success probability for the three models as given by equations 5, 7 and 12. As we can see, in the ideal channel, a link is either up or down, with no failure, whereas in the two other

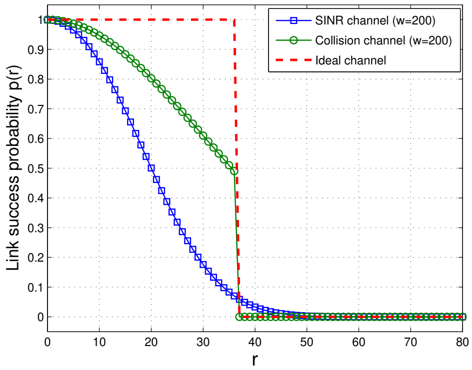


**Fig. 5:** Link success probability $p(r)$ ($S = 50000$, $\beta = 3$, $\theta = 1$, $C = 1$, $W = 1$, $\lambda_0 = 0.0035$, $\tau = 10$).

channels, links are unreliable and transmissions are always prone to failure. For the two models where interference or collisions are considered, the success probability gets more and more distant from the ideal step function as the number of interfering nodes increase. This can be seen on Figures 6(a) and 6(b) where $p(r)$ is depicted for various intensities of interfering nodes.

On Figures 6, we can observe the impact of the *Rayleigh* channel on the link success probability. In the *collision* channel, a constant transmission power $S$ has been considered and thus, we have $p(r) = 0, \forall r \geq R(S)$. In the *sinr* model study of Section 7.3, we have considered an exponential distribution for $S$ to introduce the fading phenomena. The mean of the exponential distribution has been chosen equal to the constant power $S$ considered in the other models. Randomization of $S$ has two impacts. First, it reduces $p(r)$ for values of $r$ inferior to $R(S)$ as the received signal strength may be reduced by the fading. Second, it may create some links of length $r \geq R(S)$ as the fading phenomena modeled by the exponential distribution may also increase the transmitted power $S$ compared to its mean value. The result is a curve $p(r)$ which does not show the discontinuity property at $r = R(S)$.

## 8.3 Average number of neighbors

As for the link success probability, the expected number of successful receptions for a given frame varies largely depending on the considered radio model. Figure 7 illustrates this value for the *collision* and *sinr* models as a function of the transmission power. As we can see, the expected number of correct receptions is larger in the *collision* model, around twice with the chosen numerical values, than in the *sinr* one. However, increasing the transmission power has the same effect in both models: the expected number of correct receptions increases and converges towards a constant. This differs from the *ideal* model where $\mathbb{E}[N]$ increases linearly with $S$ and diverges. From equation 8, we can state that the convergence value is $\frac{1-p}{p}$ for the *collision* model and thus independent from the node density. It is not trivial to derive this limit from equation 13 in the *sinr* model except for the particular case where $C = 0$:

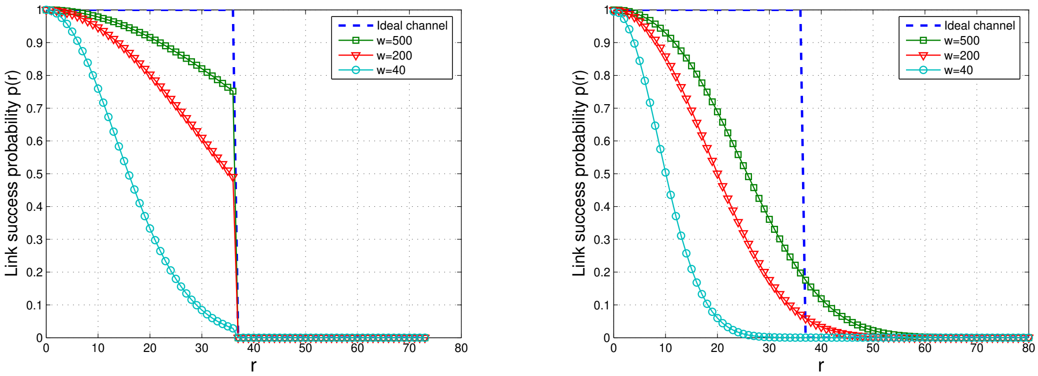


(a) *collision* model (b) *sinr* model

**Fig. 6:** Link success probability $p(r)$ ($S = 50000$, $\beta = 3$, $\theta = 1$, $C = 1$, $W = 1$, $\lambda_0 = 0.0035$, $\tau = 10$).

$$
\begin{aligned}
\mathbb{E}\left[N\right] &= \lim_{S->+\infty}(1-p)q\lambda_0 2\pi\int_0^{+\infty} p(r)rdr \\
&= (1-p)q\lambda_0 2\pi\int_0^{+\infty}\lim_{S->+\infty} p(r)rdr \\
&= (1-p)q\lambda_0 2\pi\int_0^{+\infty} e^{-\lambda_2 2\pi^2\frac{(\theta)^{\frac{2}{\beta}}r^2}{\beta sin\left(\frac{2\pi}{\beta}\right)}} rdr \\
&= \frac{(1-p)q\lambda_0}{\lambda_2}\frac{\beta sin\left(\frac{2\pi}{\beta}\right)}{2\pi(\theta)^{\frac{2}{\beta}}} \\
&= \frac{(1-p)}{p}\frac{\beta sin\left(\frac{2\pi}{\beta}\right)}{2\pi(\theta)^{\frac{2}{\beta}}}
\end{aligned}
$$

If we now consider the scalability of the neighbor discovery process, *i.e.*, the evolution of the expected number of correct receptions as a function of the node intensity $\lambda_0$, we observe radically different behaviors, as shown on Figure 8(a) and 8(b). If $\mathbb{E}\left[N\right]$ first increases with $\lambda_0$ in both cases, it then converges towards $\frac{1-p}{p}$ in the *collision* model whereas it starts decreasing towards 0 in the *sinr* one. Contrarily to the study of $\mathbb{E}\left[N\right](S)$, the asymptotic behavior of $\mathbb{E}\left[N\right](\lambda_0)$ is not similar in the two models.

To conclude with this comparison, and as a snapshot of the impact of collisions and interference on the behavior of a radio link, and by extension any communication protocol, Figure 9 illustrates the scalability of $\mathbb{E}\left[N\right]$ and its asymptotic behavior in the three studied radio channel models. The observed differences clearly highlight the importance of a correct radio modeling during the design and study of a communication protocol.

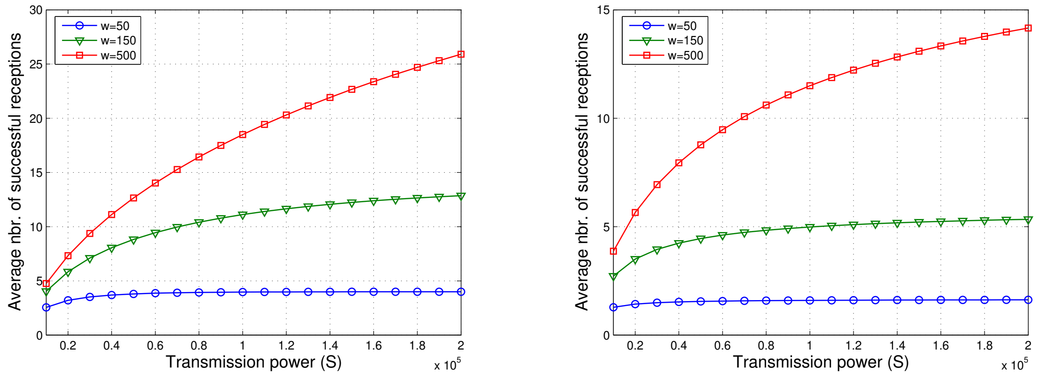


(a) *collision* model (b) *sinr* model

**Fig. 7:** Average nbr. of discovered neighbors ($\lambda_0 = 0.0035$, $\beta = 3$, $\theta = 1$, $C = 1$, $\tau = 10$).

# 9 Dimensioning of hello protocols

As an example of application, we propose to study the dimensioning of the energy aware `Hello` protocol described in Section 3. The goal of dimensioning is to choose correctly the protocol parameters in order to adapt the link probability success between a node and its neighbors according to the application constraints, while minimizing the protocol energy consumption. A real scenario stemming from the *CAPNET* project is proposed as a case study.

## 9.1 Probability of node discovery

In real world deployments, we can expect a sensor network or delay-tolerant network application to have some constraints on the neighbor discovery process. Not necessarily hard constraints, but probabilistic or statistical constraints such as: "*all nodes at distance at most 10 meters must be discovered as neighbors with high probability*" or "*node at distance more than 15 meters must not be seen as neighbors*. Mobility may also add some constraints on the neighbor discovery process: "*all nodes remaining more than 30s at less than 10 meters should be discovered as neighbors with high probability*". The study done in Section 7 offers the opportunity to dimension the protocol to match this type of constraints.

Given the use of *sleep* periods, the link success probability is not enough to determine the correct reception of a `Hello` packet by a node. Indeed, if the considered receiver is not active, the packet is lost. Thus the probability of link success, $p(r)$, computed in Section 7 has to be refined in order to cope with inactivity periods. Given a transmitter $x$ and a receiver $y$ such that $\|x - y\| = r$, we define the probability of node discovery $p_d(r)$ as the probability that $y$ correctly receives the `Hello` packet from $x$ while in *listen* mode. This probability depends on the probability of link success $p(r)$ and the probability that $y$ is listening to the medium:

$$p_d(r) = \frac{w - \tau}{w + s}\ p(r) \tag{14}$$

Given this definition, if the application requires all nodes within distance at most $L$ to be discovered

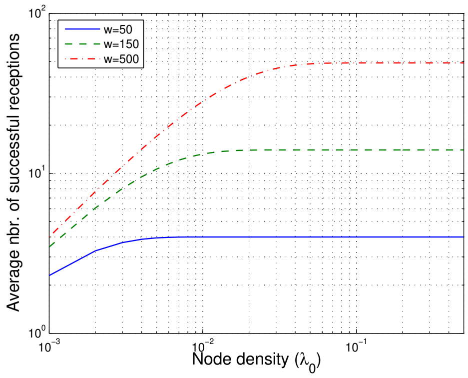


(a) *collision* model

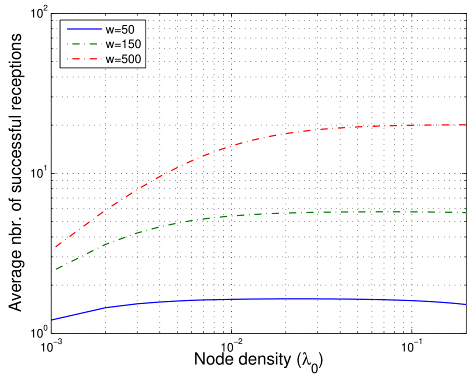


(b) *sinr* model

**Fig. 8:** Impact of $\lambda_0$ on the average nbr. of successful receptions ($S = 50000$, $\beta = 3$, $\theta = 1$, $C = 1$, $W = 1$, $\tau = 10$, $\mu = \frac{1}{S}$).

with probability a least $p_{min}$, we must select $w$, $s$ and $S$ in order to satisfy the condition: $p_d(L) \geq p_{min}$.

In order to cope with constraints bound to mobility, we can also be interested in the number of times a `Hello` packet must be sent by $x$ before its correct reception by $y$. We denote by $\varrho$ the random variable representing the first time $y$ correctly receives the `Hello` packet. If the successive transmissions were independent, $\varrho$ would follow a discrete geometric law defined as follows:

$$\mathbb{P}(\varrho = k) \; = \; p_d(r)\,(1 - p_d(r))^{k-1} \quad \text{and} \quad \mathbb{E}[\varrho] = \frac{1}{p_d(r)}.$$

Unfortunately, the successive transmissions may not be independent. Indeed, if a transmission fails, it indicates the presence of some emitting nodes in the neighborhood which have interfered. And if the emitters are the same between the successive transmissions, it induces a correlation between the link success probability of each attempt. This correlation is such that the distribution of $\varrho$ is not a geometric law. However, if the intensity of interfering nodes is not excessively high compare to the intensity of nodes (all the nodes), the geometric law can be used as a good approximation.

## 9.2 *Case study: the* CAPNET *project*

As a case study, we consider the example of the *CAPNET* project. In this project, it is planned to equip all students of the French engineer school *INSA de Lyon* with contact loggers. The task of these sensor is to periodically discover all the students present in their owner vicinity, to log this information and periodically upload it in a database through the relay of base stations. The collected data should be useful to study graphs of human interaction as well as students mobility. In the big lines, this project is similar to the pocket-switched network experience that took place at the INFOCOM 2005 conference in Miami, USA.

In the *CAPNET* project, one objective is to have the experiment last for several weeks. It induces a very strong constraint on the energy consumption of the neighborhood discovery process. Moreover, the

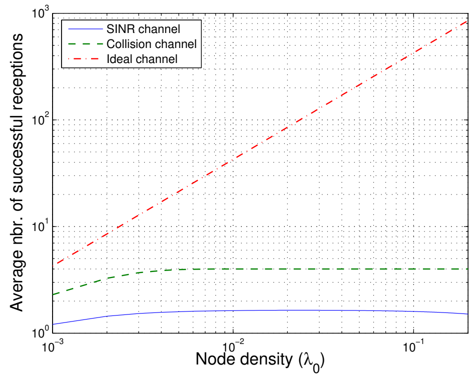


**Fig. 9:** Average nbr. of successful receptions ($S = 50000$, $\beta = 3$, $\theta = 1$, $C = 1$, $W = 1$, $\lambda_0 = 0.0035$, $\tau = 10$).

technical requirements of the project are such that a contact must be logged whenever two sensors are closer than $10$ meters for a period superior or equal to $30$ seconds.

### 9.2.1 Description of the sensors and assumptions

The sensors which are used in the *CAPNET* experiment are built with the *CC1100* communication chipset (8). The *CC1100* is a RF transceiver characterized by a low power consumption and effective radio performances. The main characteristics of this transceiver are presented in Table 1.

| Parameters | Values |
|---|---|
| Transmission power (dBm) | from $-30$ to $10$ |
| Sensitivity (dBm) | from $-88$ to $-110$ |
| Frequency (Mhz) | 400 / 800 / 900 |
| Data rate (kbps) | from $1, 2$ to $500$ |
| TX energy consumption (mA) | from $10$ to $29$ |
| RX energy consumption (mA) | from $14, 2$ to $15, 4$ |

**Tab. 1:** *CC1100* characteristics (8).

We make the following assumptions given by the experiment constraints. We consider the different available transmission powers (from $-30$ to $10dBm$) with a sensitivity threshold equal to $-88dBm$ and a radio frequency of $900Mhz$. We suppose an average presence of $5$ nodes per $20m^2$ which yields to a density $\lambda_0 = 0.0125$. We assume that the size of the `Hello` packets is $18$ bytes and that the data rate of the sensors is $2.4$kbps. The transmission of one hello packet has a duration of $\tau = 60ms$.

In Table 2, we present the maximal communication range, $R(S)$, associated to the various available transmission powers. The average number of nodes present in the disc of radius $R(S)$ and the energy consumption for the transmit mode are also presented. We assume that the average energy consumption in receive mode is $14, 8mA$.

Finally, given that nodes (*i.e.,* the students) are mobile, we wish to dimension the `Hello` protocol

| **S** (dBm) | -30 | -20 | -10 | 0 | 10 |
|---|---|---|---|---|---|
| **R(S)** (m) | 7,63 | 16,44 | 35,41 | 76,29 | 164,35 |
| **Nbr. of nodes** | 2,28 | 10,6 | 49,21 | 228,44 | 1060,17 |
| **TX** (mA) | 10 | 12 | 14 | 16 | 30 |

**Tab. 2:** Sensors parameters.

to guarantee the discovery of a node located at a distance below $L = 10m$ during at least $30s$ with a probability of $90\%$. According to the results of Table 2, we can already restrict ourselves to a transmission power $S \geq -20dBm$.

### 9.2.2 Hello protocol's dimensioning

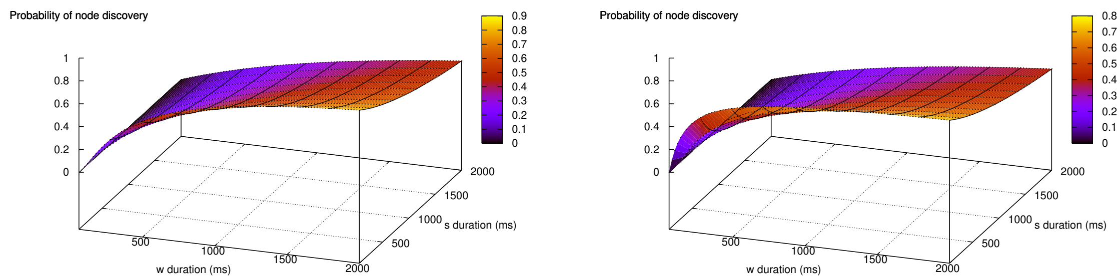


(a) *Collision* model (b) *SINR* model

**Fig. 10:** Probability of node discovery ($S = -20dBm$, $r = 10m$, $\lambda_0 = 0.0125$, $\theta = -88dBm$, $\tau = 60ms$, $\delta = 1$, $\beta = 3$, $C = 1$)

The probability of node discovery (see Eq. 14) is depicted on Figure 10 for different sizes of $w$ and $s$. On Figure 10(a), the probability of node discovery is plotted according to the *collision* model, while on Figure 10(b), we consider the *sinr* model. We notice on both figures that the probability of node discovery is raised for a high $w$ duration and a short $s$ period. Indeed, increasing $w$ reduces the number of interfering nodes and thus increases the link success probability. In addition, decreasing $s$ reduces the probability for the receiving node to be in the inactive state and thus increases the probability to discover the emitter.

On Figure 11(a) the probability of node discovery is depicted for the *collision* model and the *sinr* one according to different transmission powers ranging from $-20dBm$ to $0dBm$. The *collision* model is depicted for only one transmission power as its link success probability is not function of this parameter. We can observe from the obtained results that an increase of the transmission power raises the probability of node discovery in the *sinr* model. For example with a transmission power of $-20dBm$, this probability remains lower than $0.8$. However if we increase the transmission power to $-10dBm$, this probability is raised above $0.9$. Thus, when dimensioning the `Hello` protocol, both the transmission power and the periods $w$ and $s$ have to be well defined.

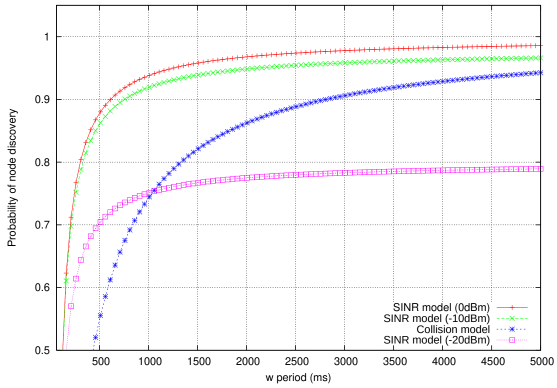


(a) Probability of node discovery ($s = 0$).

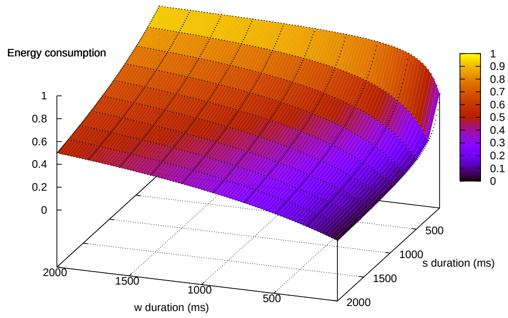


(b) Energy consumption.

**Fig. 11:** Probability of node discovery according to $S$ / *SINR* versus *Collision* model. ($r = 10m$, $\lambda_0 = 0.0125$, $\theta = -88dBm$, $\tau = 60ms$, $\delta = 1$, $\beta = 3$, $C = 1$)

Finally, the normalized energy consumption is plotted on Figure 11(b) for varying sizes of $w$ and $s$. This normalized energy is defined as : $e(w, s) = \frac{w}{w+s}$. As expected, we notice that the energy consumption increases with $w$ and decreases as the inactivity period $s$ increases. It is then important to choose the adequate size for $w$ and $s$ to ensure a low energy consumption.

| **Models** | **SINR** | | | | | **Collision** |
|---|---|---|---|---|---|---|
| | -20dBm | -10dBm | 0dBm | 10dBm | 20dBm | |
| $w$ **period (ms)** | - | 9900 | 9840 | 9900 | 9900 | 9960 |
| $s$ **period (ms)** | - | 790 | 1000 | 1030 | 1030 | 800 |
| **Normalized energy** | - | 0.92 | 0.90 | 0.90 | 0.90 | 0.92 |

**Tab. 3:** Hello protocol parameters dimensioning. ($r = 10m$, $\lambda_0 = 0.0125$, $\theta = -88dBm$, $\tau = 60ms$, $\delta = 1$, $\beta = 3$, $C = 1$)

In order to dimension the parameters, we resolve numerically the equation 14. We make the size of $w$ vary and for each considered value, we seek the optimal size of $s$ such that the constraint $p_d(10) \geq 0.9$ is respected. Many configurations are then obtained and the one which minimizes the normalized energy consumption is selected. This process is repeated for the *collision* model as well as for the *sinr* model with a transmission power ranging from $-20dBm$ to $20dBm$. The obtained results are summarized on Table 3. As already seen in Figure 11(a), the use of a transmission power $S = -20dBm$ does not allow to meet the dimensioning requirements in the *sinr* model. We also observe that the use of a transmission power higher or equal to $-10dBm$ guarantees a probability of node discovery higher than $0.9$. Thus, we must consider $S \geq -10dBm$.

To choose between the acceptable values of $S$, we look more closely to the protocol energy consumption. We refine the normalized energy consumption $e_S(w, s)$ definition to consider the transmission power:

$$e_S(w,s) = \frac{P_{rx}w + P_{tx}(S)\tau}{w+s}$$

where $P_{rx} = 14,8mA$ and $P_{tx}(S)$ values are taken from Table 2. Given he numerical values of Table 3, the set of parameters that finally minimizes the energy consumption of the `Hello` protocol is $S = 0dBm$ , $w = 9840ms$ and $s = 1000ms$.

## 10 Conclusion

In this paper, we have analytically analyzed the impact of collisions and interference on two `Hello` protocols in the context of multi-hop wireless networks. We have computed the link success probability as well as the expected number of nodes that correctly receive a `Hello` packet in three radio channel models that handle interference in very different ways. Using this analysis, we have shown that if the neighbor discovery process is asymptotically equivalent in the three models, it offers very different behaviors locally in time. In particular, the scalability of the process varies depending on the way interference is handled. Finally, we have proposed a methodology to dimension `Hello` protocol parameters regarding both application constraints and energy consumption.

Several parts of this study are open to extensions. First, the radio channel model could still be refined. For example, shadowing has not been considered. Fading could also be better modeled using generic laws as the *Nakagami* functions family. More important, the condition imposed by $\theta$ on the *sinr* for a safe reception corresponds to an ideal model and does not correspond to realistic conditions. In a more realistic perspective, transmissions suffer errors as a function of their *sinr* and their modulation. This is modeled by a *bit error rate* (*ber*) which introduces more uncertainty in the link success probability study. This extensions is very promising as up to now, very few works (15) have considered the modulation and the *ber* in the study of network and communication protocol properties.

Another interesting extension corresponds to the consideration of a *carrier sense* mechanism in the modeling of the `Hello` protocol execution. This is not trivial as the point process associated to the simultaneous emitters can no more be modeled by a Poisson point process. It can however be modeled by a Matern Hard-core process. This modeling has recently been proposed in (24) in the context of dense 802.11 networks and should be extended to sensor networks.

# References

[1] G. Alonso, E. Kranakis, C. Sawchuk, R. Wattenhofer, and P. Widmayer. Randomized protocols for node discovery in ad-hoc multichannel broadcast networks. In *Conference on Adhoc Networks and Wireless (ADHOCNOW)*, Montreal, Canada, October 2003.

[2] G. Alonso, E. Kranakis, R. Wattenhofer, and P. Widmayer. Probabilistic protocols for node discovery in ad-hoc, single broadcast channel networks. In *International Parallel and Distributed Processing Symposium (IPDPS)*, Nice, France, April 2003.

[3] F. Baccelli and B. Blaszczyszyn. On a coverage process ranging from the boolean model to the poisson voronoi tessellation, with applications to wireless communications. *Advances in Applied Probability*, 33:293–323, 2001.

[4] F. Baccelli, B. Błaszczyszyn, and P. Mühlethaler. An aloha protocol for multihop mobile wireless networks. *IEEE Transactions on Information Theory*, 52(2):421–436, 2006.

[5] F. Baccelli, B. Blaszczyszyn, and F. Tournois. Spatial averages of coverage characteristics in large cdma networks. *Wireless Networks*, 8(6):569–586, 2002.

[6] E. Ben Hamida, G. Chelius, and E. Fleury. Revisiting neighbor discovery with interferences consideration. In *Third International Workshop on Performance Evaluation of Wireless Ad Hoc, Sensor, and Ubiquitous Networks (PE-WASUN)*, Torremolinos, Spain, October 2006. ACM.

[7] P. Bose, P. Morin, I. Stojmenovic, and J. Urrutia. Routing with guaranteed delivery in ad hoc wireless networks. *Wireless Networks*, 7:609–616, 2001.

[8] CC1100, 2006. http://www.chipcon.com.

[9] T. Clausen and P. Jacquet. Optimized link state routing protocol (olsr). Technical Report RFC3626, IETF, October 2003.

[10] O. Dousse, F. Baccelli, and P. Thiran. Impact of interferences on connectivity of ad hoc networks. *IEEE/ACM Transactions on Networking*, 13(2):425–436, 2005.

[11] O. Dousse, M. Franceschetti, and P. Thiran. The costly path from percolation to full connectivity. In *Allerton Conference on Communication, Control and Computing*, Monticello, USA, October 2004.

[12] O. Dousse and P. Thiran. Connectivity vs capacity in dense ad hoc networks. In *Conference on Computer Communications (INFOCOM)*, Hong Kong, China, March 2004. IEEE.

[13] M. Franceschetti, O. Dousse, D. Tse, and P. Thiran. Closing the gap in the capacity of wireless networks via percolation theory. *IEEE Transactions on Information Theory*, 53(3):1009–1018, 2007.

[14] H. T. Friis. A note on a simple transmission formula. *Proceedings of the IRE*, 41:254–256, May 1946.

[15] J-M. Gorce, R. Zhang, and H. Parvery. Impact of radio link unreliability on the connectivity of wireless sensor networks. *EURASIP Journal on Wireless Communications and Networking*, 2007:Article ID 19196, 16 pages, 2007.

[16] P. Gupta and P. Kumar. Capacity of wireless networks. *IEEE Transactions on Information Theory*, 46(2):388–404, 2000.

[17] P. Hui, A. Chaintreau, J. Scott, R. Glass, J. Crowcroft, and C. Diot. Pocket switched networks and human mobility in conference environments. In *SIGCOMM*, Philadelphia, USA, August 2005. ACM.

[18] S. Jain, K. Fall, and R. Patra. Routing in a delay tolerant network. In *SIGCOMM*, Portland, USA, September 2004. ACM.

[19] G. Jakllari, W. Luo, and S. Krishnamurthy. An integrated neighbor discovery and mac protocol for ad hoc networks using directional antennas. In *Symposium on a World of Wireless, Mobile and Multimedia Networks (WOWMOM)*, Taormina, Italy, June 2005. IEEE.

[20] M. Kim, D. Kotz, and S. Kim. Extracting a mobility model from real user traces. In *Conference on Computer Communications (INFOCOM)*, Barcelona, Spain, April 2006. IEEE.

[21] L. Kleinrock and V. Takagi. Optimal transmission ranges for randomly distributed packet radio terminals. *IEEE Transactions on Communications*, 32(3):246–257, March 1984.

[22] F. Kuo. The aloha system. *ACM SIGCOMM Computer Communication Review*, 25(1):41–44, 1995.

[23] M. McGlynn and S. Borbash. Birthday protocols for low energy deployment and flexible neighbor discovery in ad hoc wireless networks. In *International Symposium on Mobile Ad Hoc Networking and Computing (MobiHoc)*, Long Beach, USA, October 2001. ACM.

[24] H.Q. Nguyen, F. Baccelli, and D. Kofman. A stochastic geometry analysis of dense ieee 802.11 networks. In *Conference on Computer Communications (INFOCOM)*, Anchorage, USA, May 2007. IEEE.

[25] C. Perkins, E. Belding-Royer, and S. Das. Ad hoc on-demand distance vector (aodv) routing. Technical Report RFC3561, IETF, July 2003.

[26] D. Stoyan, W. Kendall, and J. Mecke. *Stochastic Geometry and Its Applications, 2nd Edition*. John Wiley and Sons Ltd, Chichester, UK, 1996.

[27] S. Vasudevan, J. Kurose, and D. Towsley. On neighbor discovery in wireless networks with directional antennas. In *Conference on Computer Communications (INFOCOM)*, Miami, USA, March 2005. IEEE.

[28] Sergio Verdú. *Multiuser Detection*. Cambridge University Press, 1998.